GCA TECHNICAL REPORT 63-7-G

GEOPHYSICS CORPORATION OF AMERICA
Bedford, Massachusetts

FINAL REPORT

Covering the period 29 March 1963 - 30 September 1963

Project Director
Richard F. K. Herzog

Principal Scientist
Helmut J. Liebl

Prepared for

Jet Propulsion Laboratory
California Institute of Technology
Pasadena, California

SPUTTERING ION SOURCE

FINAL REPORT

THIRD PHASE

SUB CONTRACT NO. 950576

under NAS 7-100

TABLE OF CONTENTS

SECTION 1

INTRODUCTION

The first phase of the work consisted in the design, construction and assembly of a novel ion source for solids, whereby the sample is bombarded with an intense beam of fast noble gas ions, which results in sputtering of the sample material. A fraction of the sputtered material was expected to be ionized. These ions can be accelerated and analyzed in a mass spectrometer. A final report covering the first phase was submitted to JPL on 28 January 1962.

The second phase of the work involved the testing of the ion source with particular emphasis on operational performance and applicability to the qualitative analysis of different types of solids. A final report covering the second phase was submitted to JPL on 15 December 1962.

The third phase of the work, which is now completed, dealt mainly with improvements of the source and power supply and the applicability of the ion source for the quantitative analysis of solids.

SECTION 2

MODIFICATION OF THE APPARATUS

2.1 GENERAL

The first task was the modification and improvement of the ion source built under JPL Contract No. 950118, including the associated power supply, with the aim to permit operation at higher energies of the primary beam, to increase the density of the bombarding ion beam and to reduce its cross section.

Operation of the ion source constructed in the first phase of the investigatio was limited to a beam energy below 15 kv because of flashovers which occured between the duoplasmatron anode and the ion acceleration electrode, or at the einzel lens. As a consequence of those flashovers, high voltage transients reached the duoplasmatron power supply, causing frequent component breakdowns. Therefore, the purpose of the redesign was not only to allow operation at higher voltages, but also to prevent component breakdown in case of flashover. With this aim in mind, a new duoplasmatron and power supply was built.

2.2 DUOPLASMATRON

The following considerations led to the new design: The plasma density on the axis of the duoplasmatron near the anode increases rapidly with magnetic field strength until, after passing a flat maximum it decreases slightly. In practice,

therefore, the duoplasmatron must be operated above a minimum magnetic field strength to provide maximum plasma density along the axis. In conventional duoplasmatrons, the magnetic field is produced by a solenoid of 2,000 to 7,000 ampere turns, providing a magnetic field of the order of 2,000 Oerstedt between the pole pieces. Therefore, replacement of the solenoid by a permanent magnet of equivalent strength appeared to be feasible and offered the following advantages:

(1) - No power supply for the magnetic field is needed. This is especially advantageous because the duoplasmatron operates at a high potential above ground and the power for the solenoid has to be supplied by a high voltage isolation transformer.

(2) The heat generated in the solenoid is of the same order as the heat generated by the arc; for a given cooling rate, a higher arc current can be drawn if the solenoid is replaced by a permanent magnet.

(3) Since the baffle electrode, which forms one pole of the magnetic field, operates at an electrical potential different from that of the anode, which forms the other magnetic pole, it is necessary in the case of a solenoid to have an additional air gap in the path of the magnetic flux through the iron enclosure to provide electrical insulation. For a given magnetic field strength the presence of the air gap requires additional magnetic induction. This is avoided if one chooses ceramic permanent magnetic material, which is electrically insulating.

(4) There are ceramic magnets on the market which have an exceptionally high coercive force, typically around 2,000 Oerstedt. Thus the required magnetic length is relatively small; therefore, less iron is needed, and since the ceramic

material itself is much lighter than copper, the whole assembly becomes considerably shorter and lighter than an equivalent design employing a magnet coil.

The replacement of the solenoid by a permanent magnet is considered to be an important step towards the development of a flyable model.

Figure 1 shows the new duoplasmatron in detail. The magnetic field is produced by three rings (1), consisting of Indox V, which were magnetized axially. The magnetic flux passes through the cover plate (2) into the baffle electrode (3), across the gap and through the anode holder (4) and the base plate (5) back to the magnet. All these parts are made of Armco iron and are nickel plated. The axial field generated in the gap amounts to about 7,000 gauss. The anode (6) is of copper and carries a .008 inch center hole through which the ions are extracted. The anode is pressed against the cooling plate (7), also of copper, by the magnetic force which the field exerts on the anode holder. The baffle electrode is centered and kept at the correct distance from the anode by a short tubular insulator (8), made of alumina. A copper ring (9) is brazed to the baffle electrode, and six insulated screws (10) hold the inner assembly together. The cooling plate, the insulator, the baffle electrode with the copper ring, and a teflon ring (11) carrying two gaskets enclose a circular channel (12) for the coolant. A stainless steel flange (13) carries the two filament feedthroughs (14) and the gas inlet tube (15). The filament (16) consists of platinum wire mesh. This is coated with barium carbonate prior to installation; it is subsequently reduced to barium oxide by an activation process.

The performance of the new duoplasmatron exceeded expectations.

2.3 POWER SUPPLY

Figure 2 represents a schematic of the new power supply for the duoplasmatron. The components are mounted within a cabinet with rounded corners in order to avoid corona discharges. The cabinet is insulated from ground and connected to the high voltage terminal. Therefore it has to be placed inside a grounded screen to protect the operator and to shield the other equipment against transients. A distance of four inches between cabinet and screen eliminates the possibility of flashover to ground. Due to the reduced power consumption of the new duoplasmatron, the rating of the 30 kv isolation transformer was reduced below that required previously. As a consequence of the more compact design of the power supply, the total capacitance to ground is also reduced considerably, less electrostatic energy is stored, and any internal flashovers are less energetic. No breakdown of rectifier diodes, which was the main trouble before has occured with the new power supply.

2.4 PRIMARY ION BEAM OPTICS

One of the main objectives of the new design was the increase of the operating voltage. For this purpose the distance between the ion acceleration electrode and the ion extraction hole in the duoplasmatron anode was increased to an optimum value where the ion beam just missed striking the inner wall of the opening in the apex of the acceleration electrode. This change in addition

to a careful polish of all the edges of the einzel lens components permitted the acceleration of the ion beam up to at least 25 kv.

Another objective was the reduction of the diameter of the bombarding beam. With the previous arrangement, the diameter of the primary ion beam at the target could not be reduced to less than 3 mm, mainly because of distortion by the deflection condenser. Two alternatives were available to correct this, either to rebuild the deflection condenser in a more sophisticated form, or simpler, to eliminate it completely and let the beam travel down straight to the target. In this case the target had to be tilted, so that the secondary ion optics was no longer axially symmetric. Although it was expected that this latter modification might significantly decrease the secondary ion collection efficiency, this was not the case and this design was adopted accordingly.

It was also considered desirable to operate the center electrode of the einzel lens at the same voltage as the anode of the duoplasmatron. Thus, the high voltage feedthrough, a likely source of flashovers, could be eliminated by connecting the center electrode internally with the duoplasmatron anode. This also resulted in the elimination of the voltage divider required in the previous desing; the corresponding decrease in power consumption reduced the rating of the high-voltage power supply.

However, the correct image adjustment of the einzel lens had now to be determined by experimenting with several inserts in the center electrode with different inner diameters. With the final setting, a beam diameter at the target of about one half of a millimeter has been achieved. However, this intense core of the beam is surrounded by a weak halo of scattered ions. A mask with a one millimeter hole has been mounted above the sample to prevent the halo of the beam hitting the sample.

2.5 SECONDARY ION OPTICS

Since in the new arrangement the surface of the target has to be inclined at an angle of 30 degrees to the previous vertical position, the sample holder had to be redesigned. Again, six samples can be mounted simultaneously, which are brought into the primary beam by rotation of the shaft.

A series of experiments was carried out in order to determine the optimum length of the first tubular electrode of the secondary ion optics for best ion collection efficiency. It turned out to be the same as the one used in the previous arrangement.

SECTION 3

RESULTS

3.1 ION SPUTTERED FROM PURE ELEMENTS

Complete secondary ion spectra up to mass number 350 were taken from the following elements: Al, Fe, Co, Ni, Cu, Zn, Zr, Nb, Ag, Cd, Sn, Ta, Pb.

Figure 3 is an example of a typical spectrum obtained from a pure iron sample.

The samples were made up from the purest elements available. All elements were bombarded with 10 kv argon ions.

In the following table only those ions are listed which are deduced from the major peaks; the ions known as instrumental background and the ions from elements present as impurities are omitted.

Table 1

Aluminum:

Al^{3+}, Al^{2+}, $\underline{Al^{+}}$, Al_2^{+}, Al_2O^{+}, Al_2OH^{+}, Al_3^{-}, Al_4^{-}, Al_5^{-}, Al_6^{-}, Al_7^{-}, Al_8^{-}, Al_9^{-}, Al_{10}^{-}.

Iron:

$\underline{Fe^{+}}$, FeC^{+}, FeO^{+}, $FeOH^{+}$, Fe_2^{+}, Fe_2C^{-}, Fe_2O^{-}, Fe_3^{-}, Fe_3C^{-}, Fe_3O^{-}, $Fe_3O_2^{-}$, Fe_4^{-}, Fe_4O^{-}.

Cobalt:

$\underline{Co}^{+}$, CoH^{+}, CoO^{+}, $CoOH^{+}$, $CoOH_2^{+}$, Co_2^{+}, Co_2H^{+}, Co_2C^{+}, Co_2O^{+}, Co_2OH^{+}, Co_3^{+}, Co_3H^{+}, Co_3O^{+}, Co_3OH^{+}, Co_4^{+}, Co_4O^{+}, Co_5^{+}, Co_5O^{+}.

Nickel:

$\underline{Ni}^{+}$, $NiOH^{+}$, $NiOH_2^{+}$, Ni_2^{+}, Ni_2H^{+}, Ni_2OH^{+}, Ni_3^{+}, Ni_3O^{+}, Ni_4^{+}, Ni_4O^{+}, Ni_5^{+}, Ni_5O^{+}.

Copper:

Cu^{2+}, $\underline{Cu}^{+}$, $CuOH^{+}$, $CuOH_2^{+}$, Cu_2^{+}, Cu_2H^{+}, Cu_2OH^{+}, Cu_3^{+}, Cu_3O^{+}, $Cu_3C_2^{+}$.

Zinc:

$\underline{Zn}^{+}$, ZnH^{+}, ZnO^{+}, $ZnOH^{+}$, Zn_2^{+}, Zn_2O^{+}, $Zn_2O_2^{+}$, $Zn_2O_3^{+}$, Zn_3^{+}, Zn_3O^{+}, $Zn_3O_2^{+}$.

Zirconium:

Zr^{2+}, $\underline{Zr}^{+}$, ZrH^{+}, ZrO^{+}, ZrO_2^{+}, ZrO_3^{+}, Zr_2^{+}, Zr_2O^{+}.

Niobium:

Nb^{2+}, $\underline{Nb}^{+}$, NbH^{+}, NbC^{+}, NbO^{+}, Nb_2^{+}, Nb_2H^{+}, Nb_2C^{+}, Nb_2O^{+}, Nb_3^{+}, Nb_3O^{+}.

Silver:

Ag^{2+}, $\underline{Ag}^{+}$, Ag_2^{+}, Ag_3^{+}, Ag_3O^{+}.

Cadmium:

Cd^{2+}, Cd^{+}, Cd_2^{+}, Cd_2O^{+}, Cd_2^{+}.

Tin:

Sn^{2+}, $\underline{Sn}^{+}$, Sn_2^{+}.

Tantalum:

Ta^{2+}, $\underline{Ta}^{+}$, TaO^{+}, TaO_2^{+}

Lead:

Pb^{3+}, Pb^{2+}, $\underline{Pb}^{+}$, PbO^{+}

Generally, the parent peak of the singly charged ion is by far the largest peak. The intensities of the doubly charged ions and of the diatomic ions are lower by about one order of magnitude than the intensities of the singly charged ions, and the intensities of the triply charged ions and the triatomic ions are lower by two orders of magnitude. Quadruply charged ions were not detected, however higher polymeric ions have been found, in the case of aluminum as high as Al_{10}^{+}.

A surprisingly large number of oxide and hydroxide ions have been found. It seems to be rather unlikely that these are actual constituents of the sample, since the surface layer, which might contain those components, is rapidly removed by the bombarding beam. Contamination of the bombarding argon beam by small amounts of water vapor and air might cause the production of these ions. A thorough investigation is planned with the new equipment designed especially to reduce the background.

The following table contains preliminary figures for the sensitivity of pure elements relative to iron if the samples are bombarded by 10 kv argon ions.

Table 2

Fe	1 (by definition)	Zr	0.18
Al	65	Nb	2.35
Co	0.72	Ag	0.25
Ni	0.56	Cd	1.52
Cu	0.18	Sn	0.28
Zn	0.61	Ta	0.05
		Pb	0.45

This comparison has been performed with the parent peaks only, which are due to singly charged ions. The samples were tested by keeping the primary ion beam as constant as possible and adjusting the secondary ion beam for maximum output of the mass spectrometer. Corrections were applied to compensate for the effect of different voltages used to accelerate the secondary ions. Naturally, the accuracy of this method is rather limited and the measurements will be repeated with the new source, now under development, which will permit a more direct comparison. Nevertheless, it can be seen already that the sensitivities for the majority of elements lie within one order of magnitude.

It might be expected that the relative secondary ion yields of the constituents of an alloy will differ significantly from the relative secondary ion yields obtained from pure elements. It can be argued that the probability of producing a sputtered ion rather than a sputtered neutral particle depends not only on

certain physical properties of the particle, in particular, its ionization potential, but also on certain physical or chemical properties of bulk material as a whole from which the particle originates, in particular, its work function. Fortunately, it has been found experimentally (See SECTION 3.2.6) that the composition of the supporting bulk material has only little influence on the sputtering yield and ionization of one particular component.

3.2 IONS SPUTTERED FROM ALLOYS

3.2.1 General

In order to investigate the quantitative behavior of secondary ions released from the surface of alloys, a number of certified samples were obtained from the National Bureau of Standards. These were:

Iron Alloys:

NBS Standard #444, 62.9% Fe, 0.019% Ti, 0.12% V, 20.5% Cr, 4.62% Mn, 10.1% Ni, 0.22% Co.

NBS Standard #461, 96.5% Fe, (0.01% Ti), 0.024% V, 0.13% Cr, 0.36% Mn, 1.73% Ni, 0.26% Co.

NBS Standard #465, 99.4% Fe, 0.20% Ti, 0.002% V, 0.004% Cr, 0.032% Mn, 0.026% Ni, 0.008% Co.

The sample material was supplied in the form of 7/32-inch diameter rods; from these, discs of 1/16-inch thickness were cut. The flat surfaces of the discs to be exposed to the bombarding beam of argon ions were polished.

Figure 4 is an example of a spectrum from a steel sample.

Tin Alloys:

NBS Standard #54d, 88.57% Sn, 7.04% Sb, 0.62% Pb, 3.62% Cu, 0.088% As.

NBS Standard #127A, 30.03% Sn, 0.79% Sb, 69.0% Pb, 0.004% Cu, 0.129% As.

NBS Standard #53d, 4.94% Sn, 9.92% Sb, 84.6% Pb, 0.268% Cu, 0.045% As.

These samplematerials are supplied in powder form from which [illegible] pellets were pressed.

3.2.2. Effect of sample preparation on relative spectral peak heights

The effect of sample preparation prior to mounting in the ion source was investigated with three samples of stainless steel Standard #444. After polishing with emery cloth, the first sample was wiped only with tissue paper, the second was rinsed in acetone and the third was dipped in a 50% solution of hydrochloric acid, rinsed with distilled water and dried with tank nitrogen.

The relative peak heights of iron, chromium and manganese showed no significant variation from sample to sample. It appears that any contaminating surface layer was removed in a period appreciably shorter than that required to record the spectrum.

3.2.3 Effect of bombarding period on relative spectral peak heights

mple of #444 Stainless steel was mounted and the primary beam of 5kv argon ions was switched on. After apperiod of several minutes,

which is required for adjustments, the first secondary ion spectrum was recorded; the recording was repeated every 15 minutes for a period of one hour. The relative peak amplitudes remained unchanged within the experimental limits of reproducibility. This result indicates that an equilibrium is reached within the period required for initial adjustments.

3.2.4 Effect of primary beam energy on absolute spectral peak heights

The spectrum of a sample of #444 Stainless Steel was recorded with primary beam energies varying in steps from 5 kv to 25 kv (Figure 5, curve 1), and then a second time, starting from 5 kv again (curve 2). The intensity seems to level off for Fe above 20 kv, while for Cr it continues to increase. The higher intensity at the second run may be the result of surface cleanup during the first run.

3.2.5 Effect of primary beam energy on relative sensitivities

From the run described above the sensitivities of Ni, Mn, Cr and V relative to iron were evaluated by dividing the peak height ratios by the actual relative atomic concentrations (Figure 6). It was expected that the discrimination between different elements would decrease with increasing bombarding energy (See Final Report - Second Phase - Section 4). For the elements Vanadium and Chromium, which have a much higher sensitivity than iron, the curves show indeed a slightly decreasing tendency up to about 20 kv. From there on, however they increase again. With manganese and nickel this effect is not noticeable.

One possible explanation for this behavior might be that up to about 20 kv the argon ions loose their energy close enough to the surface, so that the "apparent temperature" of the surface increases. At energies above 20 kv, they penetrate deeper into the lattice and less energy is absorbed in the surface layers, so that the "apparent temperature" decreases again.

This result indicates that one does not gain anything by using bombarding energies higher than 20 kv as far as discrimination between different elements is concerned.

3.2.6 Effect of concentration on relative sensitivities

The relative sensitivities of the main constituents in the three iron alloys were obtained from the mass spectra in the same manner as described in 3.2.5 and compared with the actual certified concentrations. The relative sensitivities thus deduced for three different concentrations are plotted in Figure 7 for 10 kv and 15 kv primary beam energy.

Generally, it seems that the relative sensitivities of each element tested so far (Ni, Cr, Co, Ti, V) deviate from the mean value by less than ±50% over the wide range of concentrations covered. The only exception is manganese, mass number 55, where on one sample a larger deviation has been found. Further experiments will be needed to explain this abnormal behavior. The isolated points, which are not connected with the curves are shifted by the instrumental background, which becomes significant at these low concentrations and tends to

increase the apparent sensitivity for minor constituents. Extension of quantitative measurements to lower concentrations will be possible with the improved design of the ion source, now under development.

Figure 8 shows a similar plot obtained from the three tin alloys. Here, the maximum deviation of the relative sensitivities of the constituents (Cu, As, Sb, Pb) lie within ±28%, with the only exception of copper at the lowest concentration of 0.00004, which again can be explained by instrumental background.

The fact that the relative sensitivities are essentially independent of the relative concentrations is of extreme importance for the performance of a quantitative analysis. The best way to perform such an analysis is to compare the mass spectra of the unknown sample with two or more calibration samples of known composition. These calibration samples should consist of the same constituents as the sample to be analysed. The concentration of the components of the calibration samples whould cover a wide range which covers the concentrations to be expected in the sample to be analysed. Naturally, before this quantitative analysis can be done, it is necessary to know approximately the composition of the sample. A qualitative mass spectrum with an evaluation of the peak heights is the first step in this direction. After the relative sensitivities of all components have been measured with the calibration samples, these figures can be applied to the unknown sample and relative concentrations of its components can be computed. Judging from the results obtained so far, it is expected that in this way the error in the measured composition can be

reduced to less than ±50%. The use of a single calibration sample is possible, if a slightly higher error is tolerable. A fair accuracy can be achieved even without any special calibration, if the relative sensitivity values of the pure elements are used for the evaluation of the mass spectra. For instance, the sensitivity ratio Ni/Fe and Co/Fe agreed perfectly, and Pb/Sn within the 50% error limit; only the sensitivity ratio of Cu/Sn as derived from pure elements was slightly below the value obtained from alloys.

3.3 IONS SPUTTERED FROM COMPOUNDS

Some preliminary runs were made in order to compare the secondary ion spectrum of a metal with that of some of its compounds. The element chosen was zirconium, and the compounds were zirconium oxide ZrO_2, zirconium oxychloride $ZrOCl_2 \cdot 8H_2O$, zirconium nitrate $Zr(NO_3)_4$, zirconium sulphate $Zr(SO_4)_2$ because this region of the mass spectrum is relatively free of instrumental background.

The pure zirconium metal was supplied in the form of a rod, 3mm in diameter, from which a short piece was cut and mounted on the sample holder. The compounds were supplied in the powder form which was pressed into pellets of 1/4 inch diameter and 1/16 inch thickness, mounted on the sample holder simultaneously with the metal.

The spectrum of the pure zirconium metal showed the peaks listed in Table 1. The Zr^+ and ZrO^+ peaks were about equally high, and about ten times as intense as the ZrO_2^+ and Zr_2^+ peaks, the Zr_2O^+ peaks were about one third as high as

the Zr_2^+ peaks. The other peaks were extremely small. Strong outgassing from the compound samples must have occurred, since the chlorine peaks appeared also in the spectrum of the pure element.

With the zirconium oxide sample the ions Zr^+, ZrO^+ and ZrO_2^+ appeared in about the same relative ratio as with the pure metal, however the intensity was reduced to about 1/10. The Zr_2^+ peaks did not appear at all, whereas, the $Zr_2O_2^+$ peaks appeared with about the same intensity as the ZrO_2^+ peaks. There was also a weak O^+ peak, but no O_2^+ peak.

The spectrum of zirconium oxychloride showed the peaks Zr^+, ZrO^+, $ZrCl^+$, Zr_2O^+ and Zr_2Cl^+ in about equal intensities. Besides these O^+, H_2O^+, O_2^+ and Cl^+ peaks appeared.

When zirconium nitrate was bombarded, it commenced to outgas so vehemently that the pressure rose considerably. Intense peaks appeared representing Zr^+, ZrO^+ and ZrO_2^+. The ZrO^+ peaks were about twice as high as the Zr^+ peaks. No N^+ peaks was found, only a weak N_2^+ peak.

With zirconium sulphate, only very weak peaks of Zr^+ and ZrO^+ were found. None of the other constituents appeared.

SECTION 4

CONCLUSION

The sputtering ion source for the analysis of solids, which was built and tested under Contract No. 950118, has been modified and improved during this phase of the contract, in order to allow operation at higher bombarding ion energies (up to 25 kv) and to reduce the diameter of the bombarded spot on the sample to about one-half millimeter.

Extensive runs have been performed to investigate whether the new ion source can be used for a quantitative analysis. The conclusion so far is that the sputtering ion source showed superior performance compared with the standard spark source in regard to precision of the analysis, and it is expected that the sputtering source will become an extremely valuable tool for solids analysis. However, the complexity of the problems and the large number of parameters involved demand still much more calibration work with a wider variety of test samples, in order to fully understand the behavior of the sputtering ion source and to evaluate the overall accuracy of this analytical method. So far, the choice of samples was seriously limited because of interference with instrumental background. The reduction of this background is the main objective of the proposed future work.

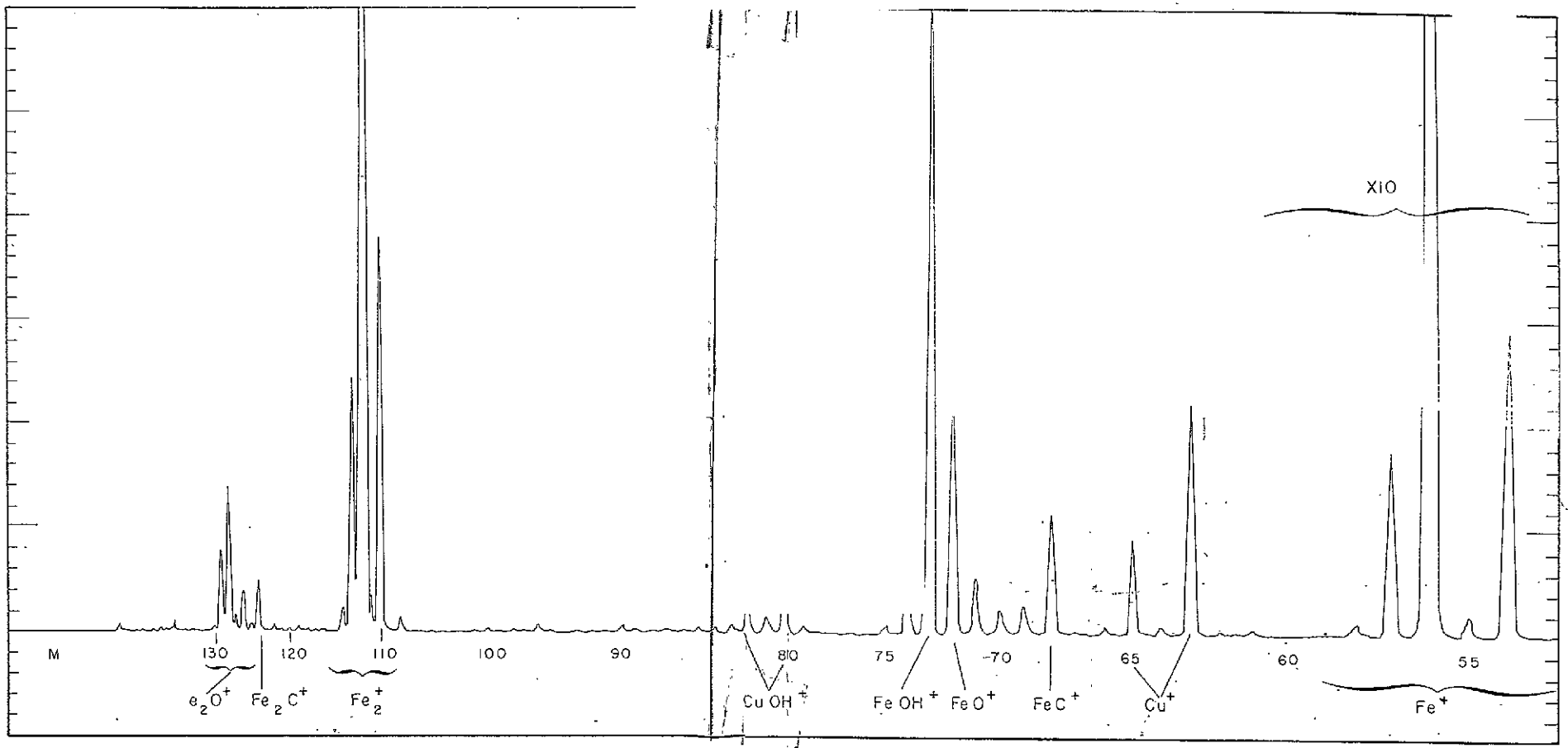

Figure 3. Part of secondary ion spectrum from a pure iron surface, bombarded with 10 kev argon ions, scanned by sweeping the accelerating field.

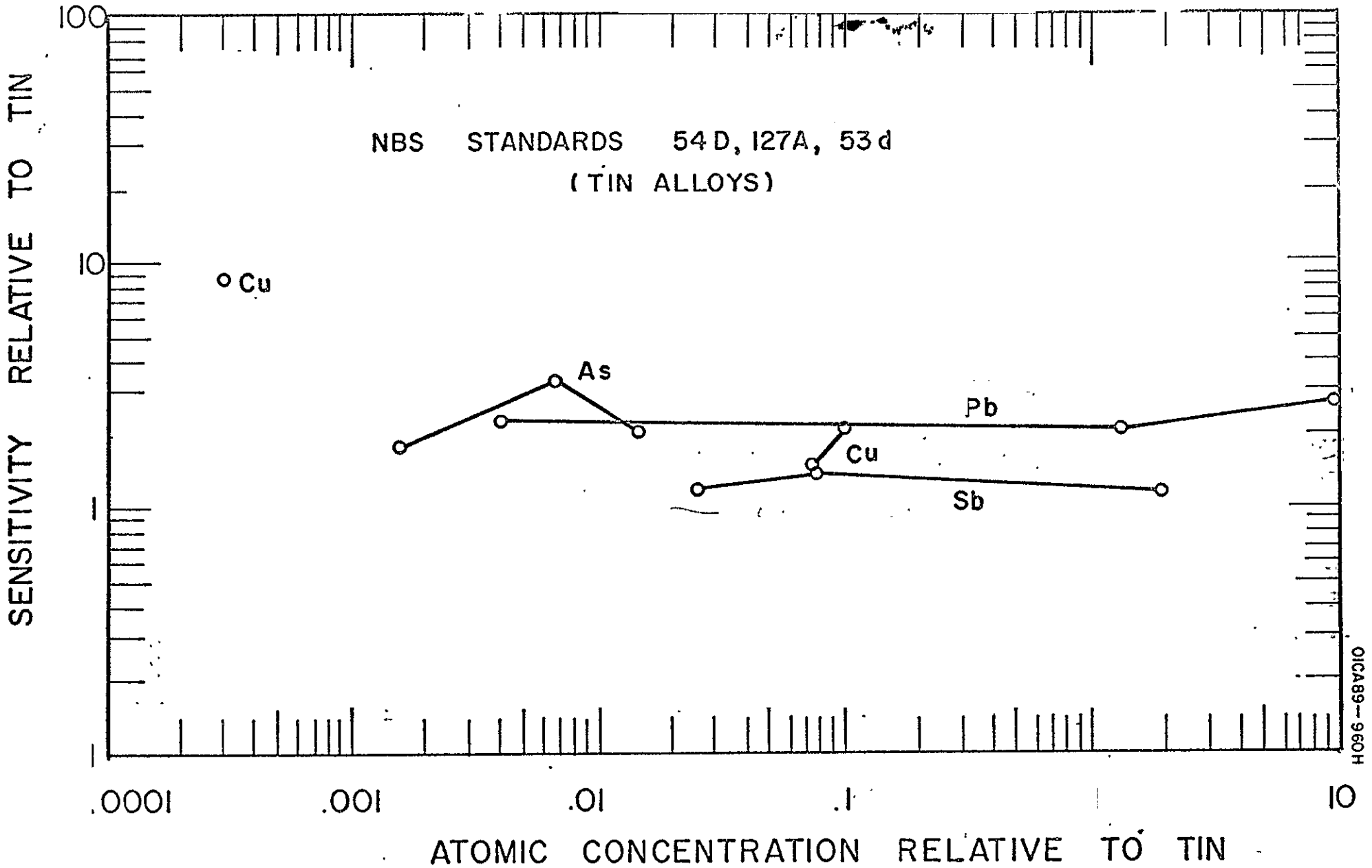

Figure 8. Effect of concentration on relative sensitivities for NBS Standards 54D, 127A and 53d (tin alloys).

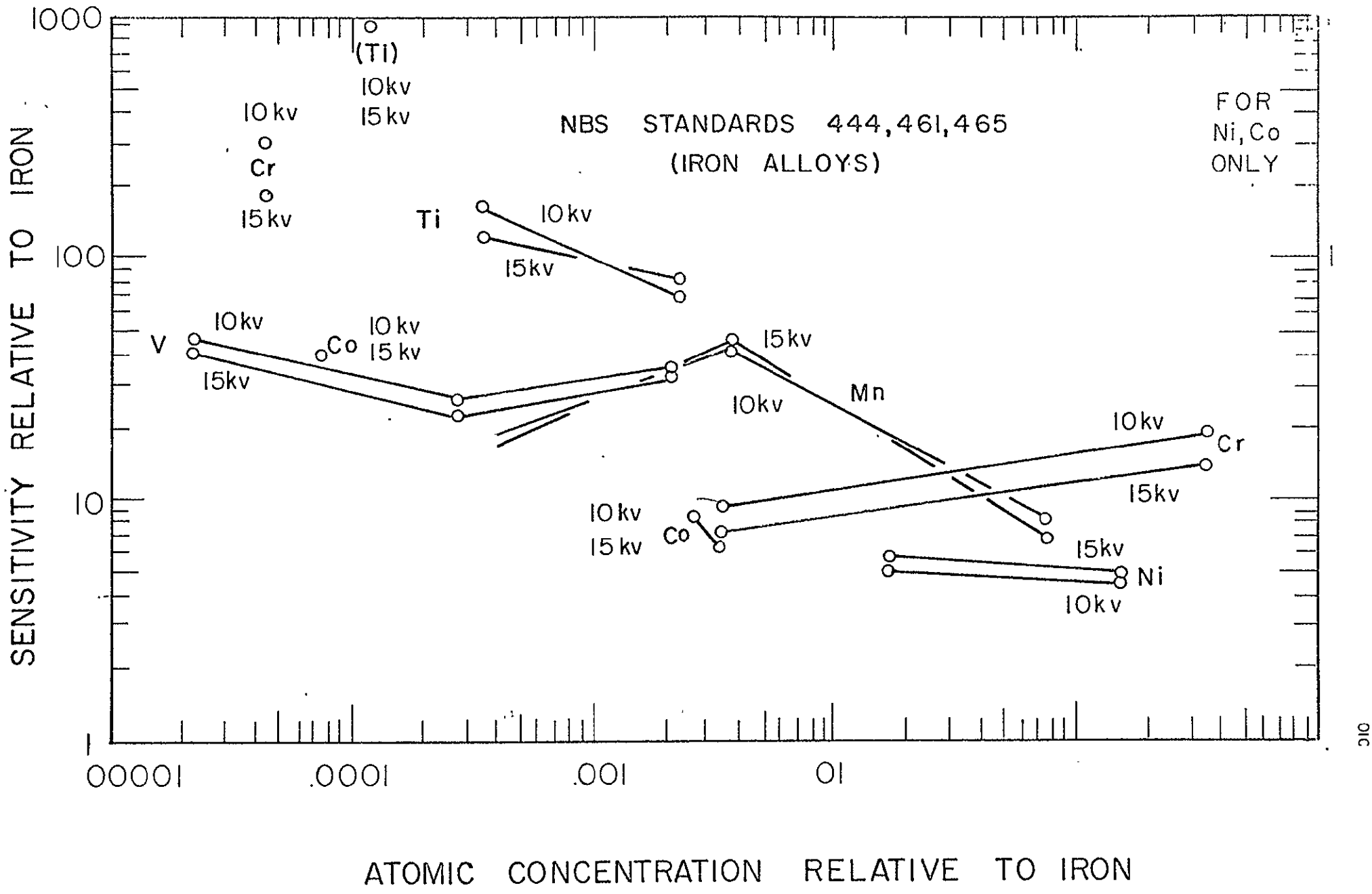

Figure 7. Effect of concentration on relative sensitivities for NBS Standards 444, 461 and 465 (Iron alloys)

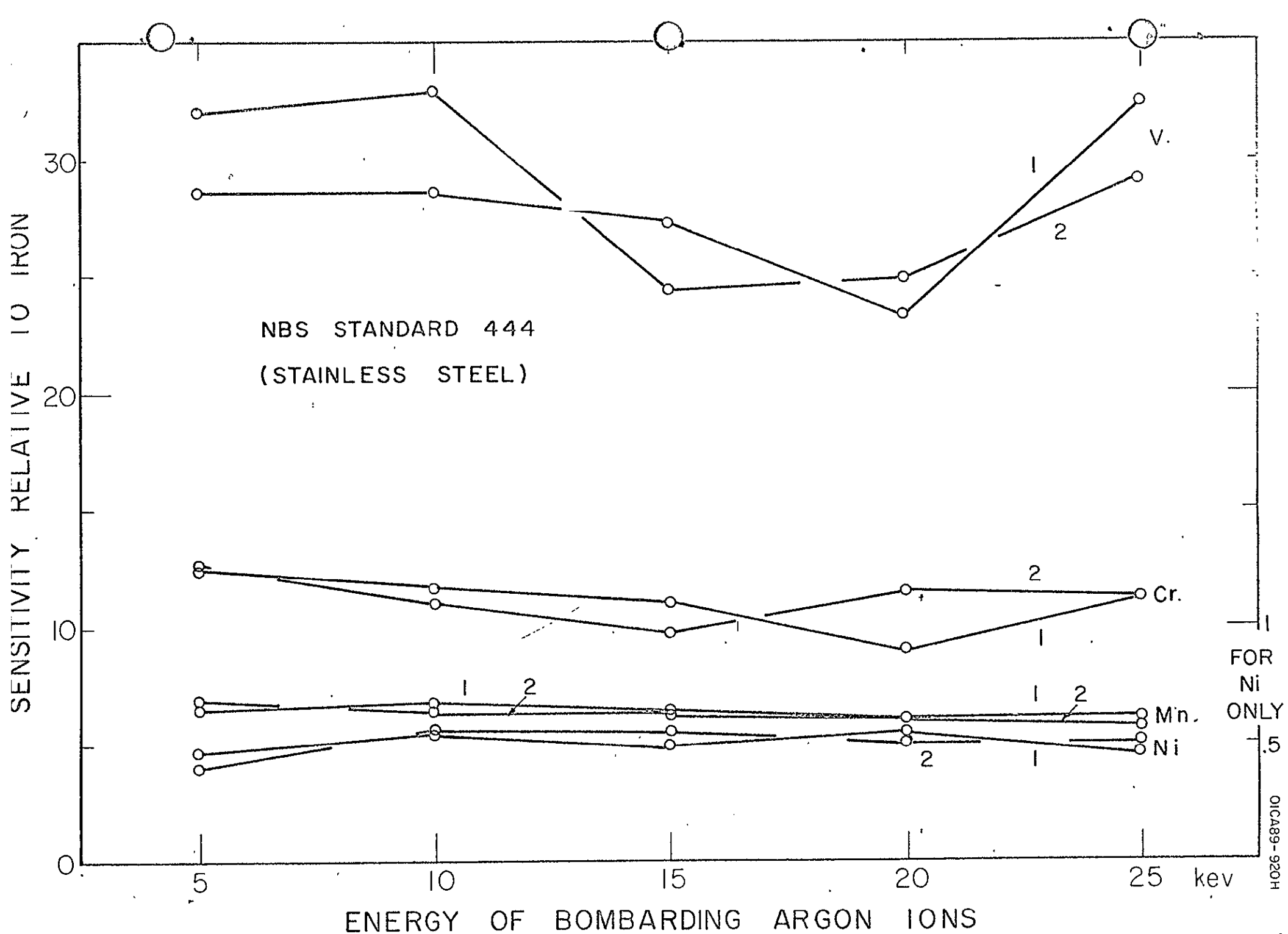

Figure 6. Effect of primary beam energy on relative spectral peak heights for NBS Standard 444 (stainless steel).

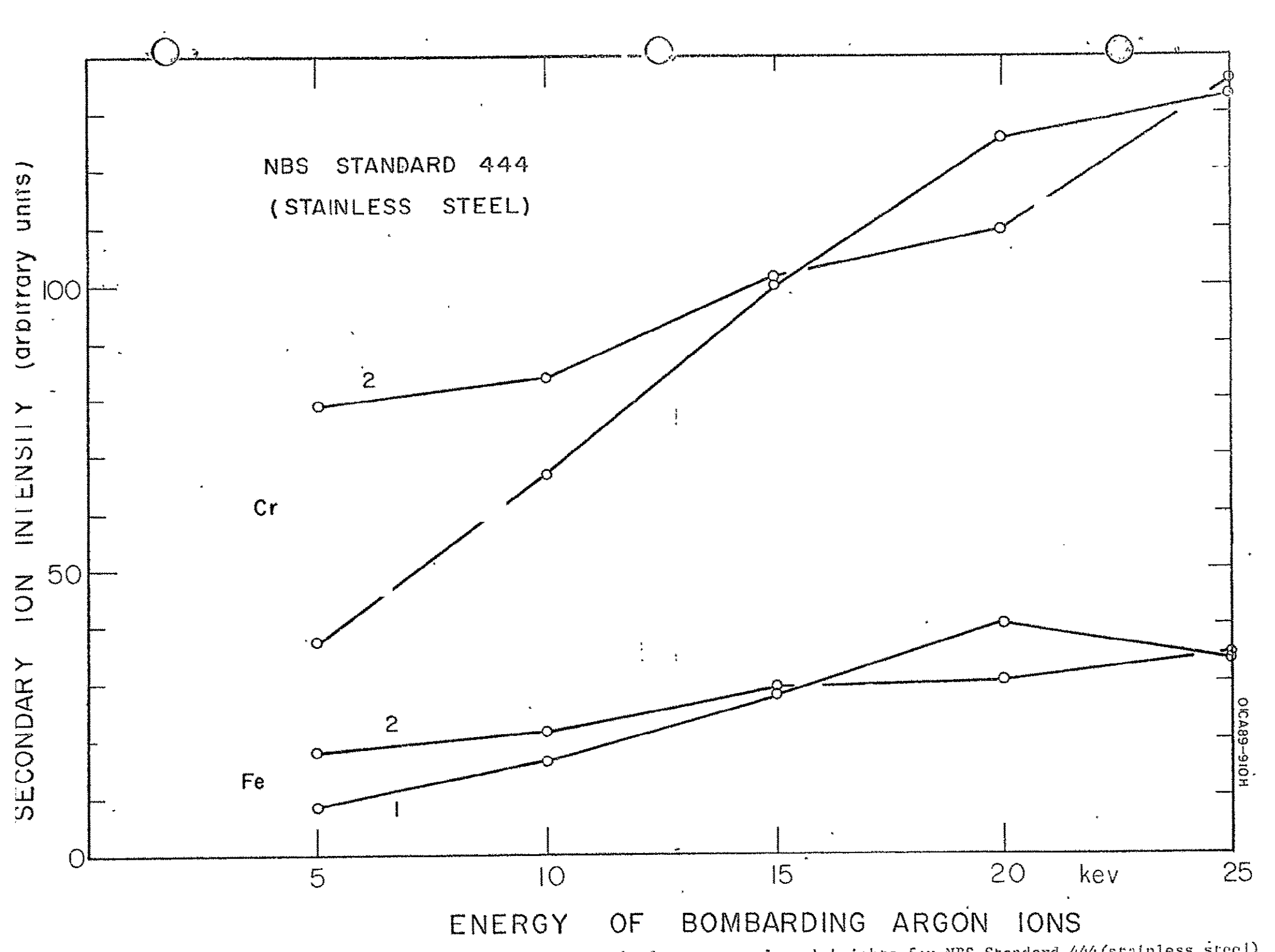

Figure 5. Effect of primary beam energy on absolute spectral peak heights for NBS Standard 444 (stainless steel)

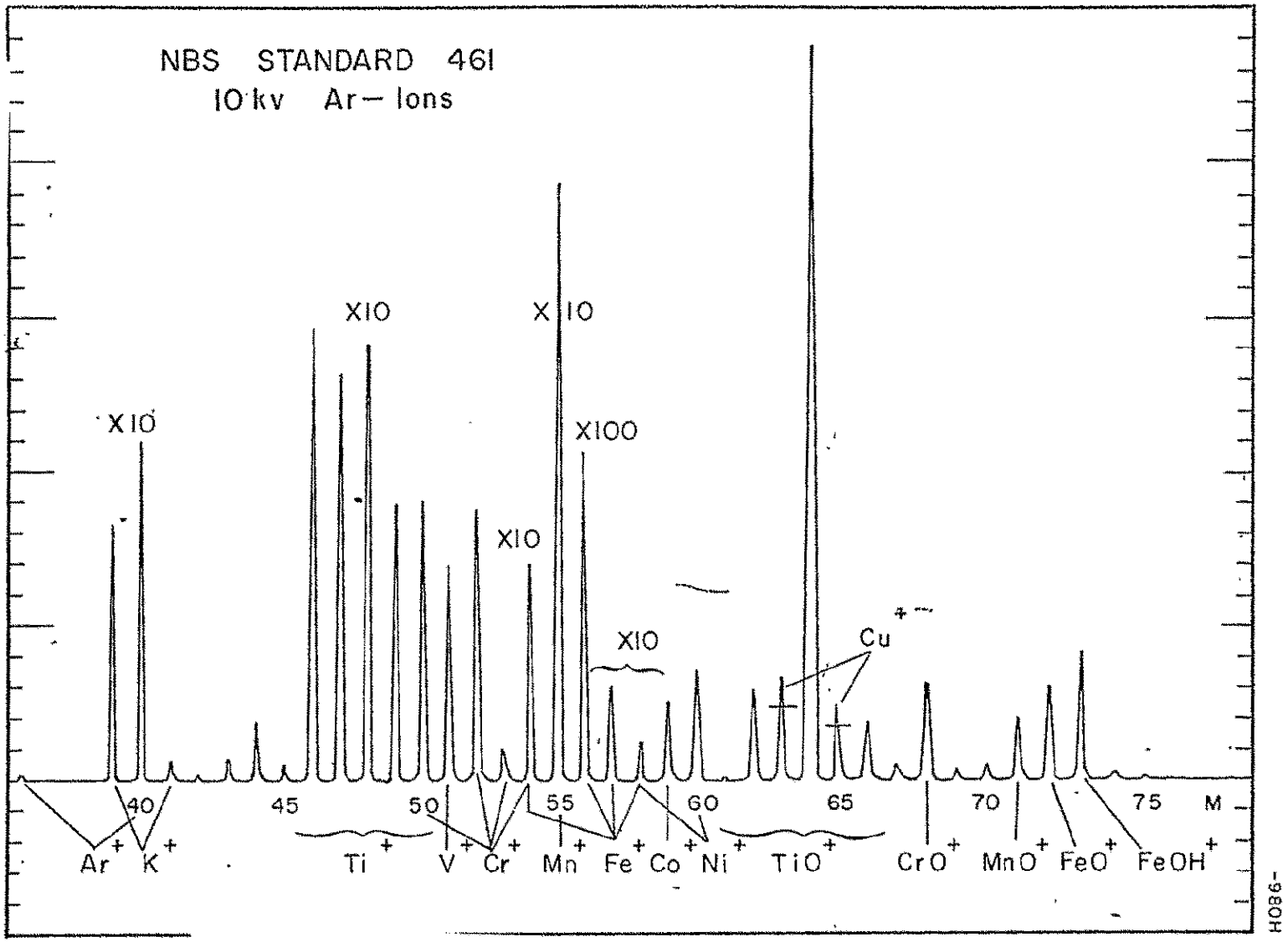

Figure 4. Part of secondary ion spectrum from a surface of NBS Standard 461 (low alloy steel) bombarded with 10 kev argon ions, scanned by sweeping the magnetic field.